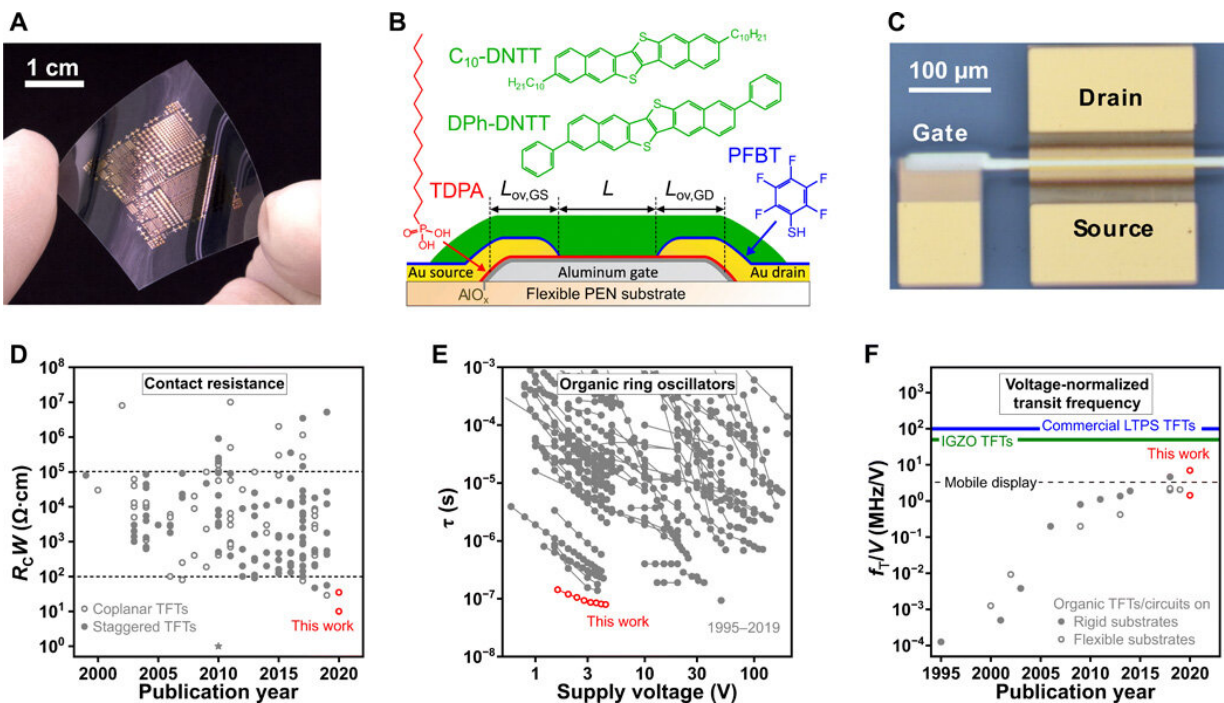


# Flexible low-voltage high-frequency organic thin-film transistors

May 29 2020, by Thamarasee Jeewandara



Flexible organic transistors with small contact resistance and high-frequency performance. (A) Photograph of organic TFTs and circuits fabricated at a maximum process temperature of 100°C on a flexible, transparent PEN substrate. (B) Schematic cross section of the TFTs and chemical structures of the organic materials used in their fabrication: n-tetradecylphosphonic acid (TDPA) used for the self-assembled monolayer (SAM) in the hybrid aluminum oxide/SAM gate dielectric, PFBT used to treat the gold source and drain contacts to reduce the contact resistance and the small-molecule organic semiconductors DPh-DNTT and C10-DNTT. (C) Photograph of a TFT having a channel length of 8  $\mu\text{m}$ , a total gate-to-contact overlap of 4  $\mu\text{m}$ , and a channel width of 200  $\mu\text{m}$ . (D) Literature overview of the width-normalized contact resistance ( $R_{\text{C}}W$ ) in

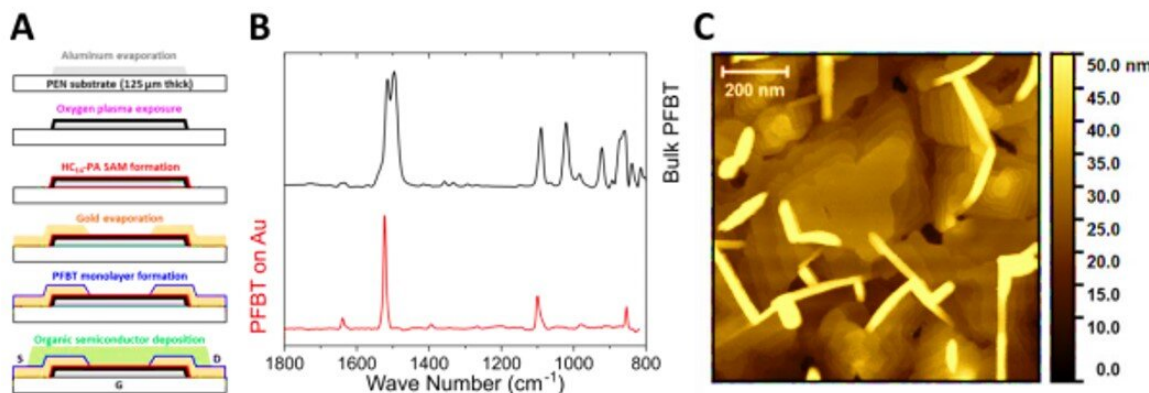
organic TFTs. The dotted lines at 102 and 105  $\Omega\cdot\text{cm}$  indicate the typical range of contact resistances reported for organic TFTs. (E) Literature overview of the signal propagation delay per stage ( $\tau$ ) of organic TFT-based ring oscillators as a function of supply voltage. (F) Literature overview of the highest voltage-normalized transit frequencies ( $f\text{T/V}$ ) of organic TFTs fabricated on rigid and flexible substrates. The solid horizontal lines indicate the voltage-normalized transit frequencies of LTPS TFTs used in smartphone displays and of state-of-the-art low-temperature-processed IGZO TFTs; the dashed line indicates approximately the minimum requirement for mobile displays (3 MHz V<sup>-1</sup>). Photo credit: James W. Borchert, Max Planck Institute for Solid State Research. Credit: *Science Advances*, doi: 10.1126/sciadv.aaz5156.

Electronic applications on unconventional substrates that require low-temperature processing methods have primarily driven the development of organic thin-film transistors (TFTs) in the past few decades. Such applications primarily require high-frequency switching (rate at which an electronic switch performs its function) or amplification at low operating voltages. However, most organic-TFT technologies show limited dynamic performance unless researchers apply high operating voltages to overcome their high contact resistances and large parasitic capacitances, i.e. a capacitance that exists between parts of electronic components or a circuit due to their proximity to each other. In this work, James W. Borchert and a team of interdisciplinary researchers in nanoscience, chemistry, quantum science and solid state research in Germany and Italy, presented low-voltage organic TFTs. The devices recorded static and dynamic performances including contact resistances as small as 10  $\Omega\cdot\text{cm}$ , on/off current ratios as large as  $10^{10}$  and transit frequencies as high as 21 MHz. The inverted coplanar TFT structure developed in this work can be readily adapted to industry-standard lithographic techniques.

Flexible electronics are presently a \$20-billion-per-year industry driven

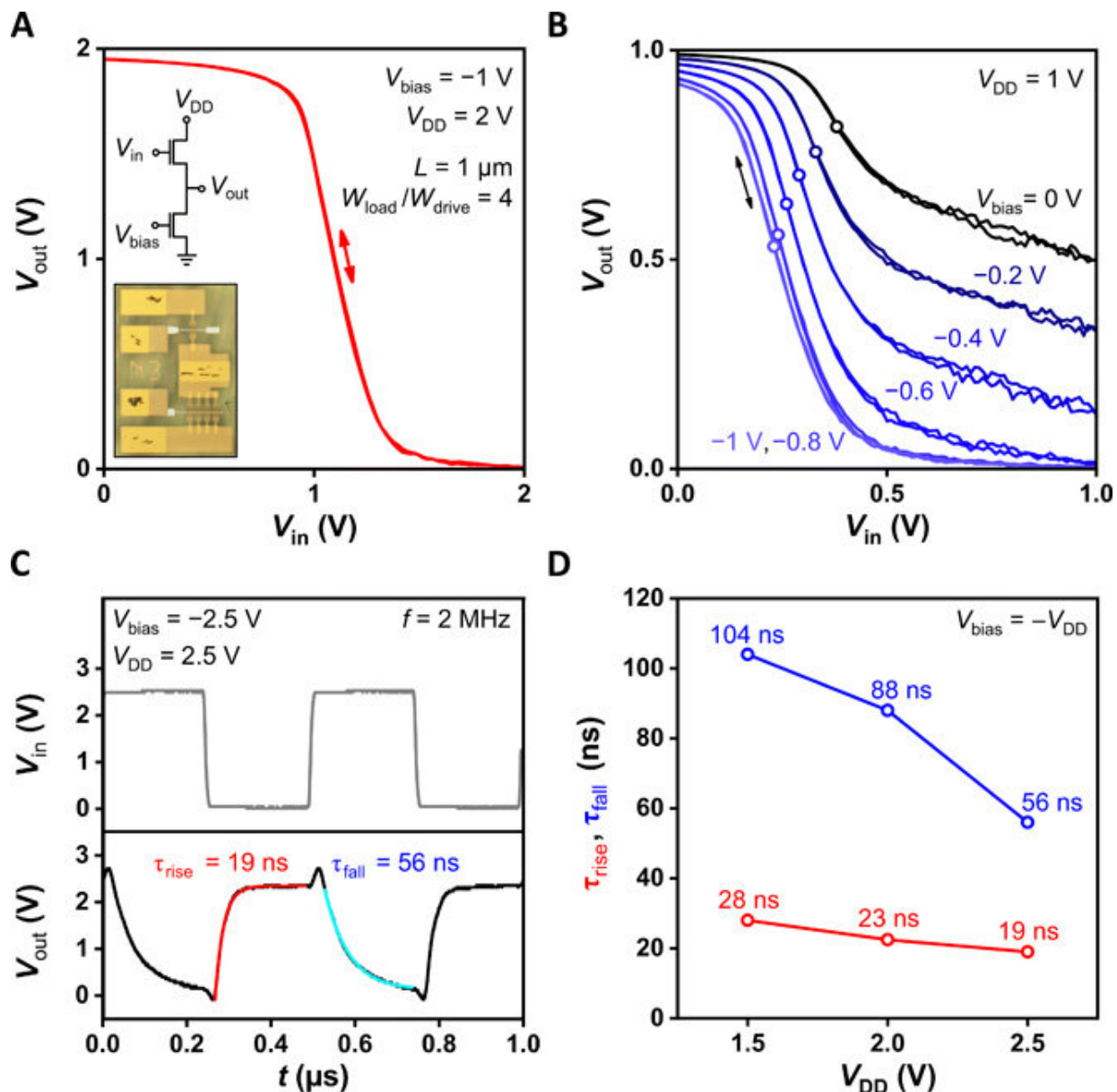
by recent trends of [active-matrix organic light-emitting diode](#) (AMOLED) smartphone displays on polyimide substrates. Among the many challenges associated with the transition, scientists must reduce the process of the thin-film transistor (TFT) technology via [low temperature polycrystalline silicon](#) (LTPS), to make it compatible with polyimide substrates, while retaining the characteristics of TFT. In this work, Borchert et al. showed the capabilities of a previously [reported method](#) to develop low-voltage organic TFTs with low contact resistance for enhanced static and dynamic performance.

They fabricated the TFTs and circuits on flexible [polyethylene naphthalate](#) (PEN) sheets with high-resolution silicon stencil marks to [pattern all device layers](#). The team combined the low contact resistance with a small channel length and small gate-to-contact overlaps to obtain record static and dynamic performances. They measured the dynamic performances of individual TFTs operating in the [saturation regime](#) using a [two-port network](#) analysis (an electrical network with two terminals connected to external circuits). Borchert et al. then measured the channel-length dependence of the transit frequency and determined a width-normalized contact resistance of  $10 \pm 2 \Omega \cdot \text{cm}$ . The experimental characteristics represented important proof-of-concepts to develop low-power flexible circuits based on organic TFTs for use in flexible AMOLED displays.



Device fabrication process and materials characterization. (A) Schematic process flow for the fabrication of bottom-gate bottom-contact (inverted coplanar) organic TFTs. All metal and semiconductor layers are deposited by thermal evaporation or sublimation in vacuum and patterned using high-resolution silicon stencil masks. (B) Infrared reflection absorption spectroscopy (IRRAS) analysis of bulk pentafluorobenzenethiol (PFBT, black) and of a chemisorbed monolayer of PFBT on a gold surface (red). (C) AFM height scan of a thin film of the organic semiconductor DPh-DNTT deposited onto a hybrid AlOx/SAM gate dielectric on a flexible PEN substrate. Credit: Science Advances, doi: 10.1126/sciadv.aaz5156

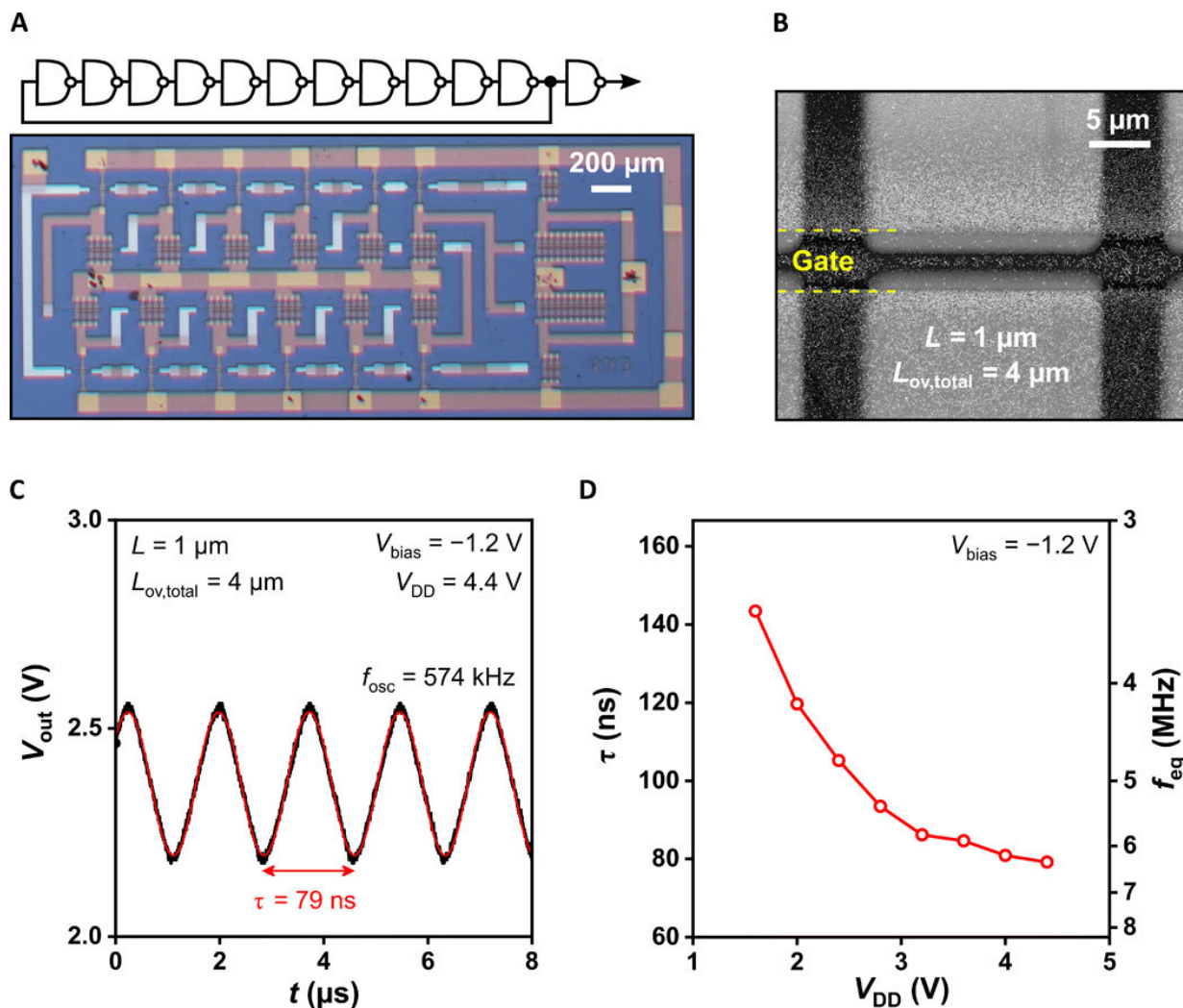
The team engineered small molecule organic semiconductors as [the active layer](#) of TFTs, on flexible polymer substrates with a channel length of 8  $\mu\text{m}$ , a gate-to-contact overlap of 4  $\mu\text{m}$  and a channel width of 200  $\mu\text{m}$ . They determined the transfer and output characteristics of TFTs based on diverse semiconductors that constituted the device. The experimental results were [similar to previous studies](#) and confirmed good reproducibility of the fabrication process. During the experiments, the scientists used two types of semiconductor materials abbreviated [DPh-DNTT](#) and [C<sub>10</sub>-DNTT](#) to form thermally stable thin film transistors (TFTs). They then observed the static and dynamic circuit characteristics using an [inverter](#) composed of DPh-DNTT based TFTs and an 11-stage [ring oscillator](#) based on C<sub>10</sub>-DNTT based TFTs. The dimensions were identical in both circuits and maintained a similar biased-load design.



Static and dynamic inverter characteristics. (A) Static transfer characteristics of an inverter based on two DPh-DNTT TFTs in a biased-load circuit design fabricated on a flexible PEN substrate for a supply voltage ( $V_{DD}$ ) of 2 V and bias voltage ( $V_{bias}$ ) of  $-1$  V. The TFTs have a channel length ( $L$ ) of  $1 \mu\text{m}$  and a total gate-to-contact overlap of  $4 \mu\text{m}$ . The insets show the circuit diagram and a photograph of the inverter. Photo credit: James W. Borchert, Max Planck Institute for Solid State Research. (B) Static transfer characteristics of the same inverter for bias voltages ranging from  $-1$  to  $0$  V. The open circles indicate the trip voltage. (C) Dynamic characteristics of the inverter in response to a square-

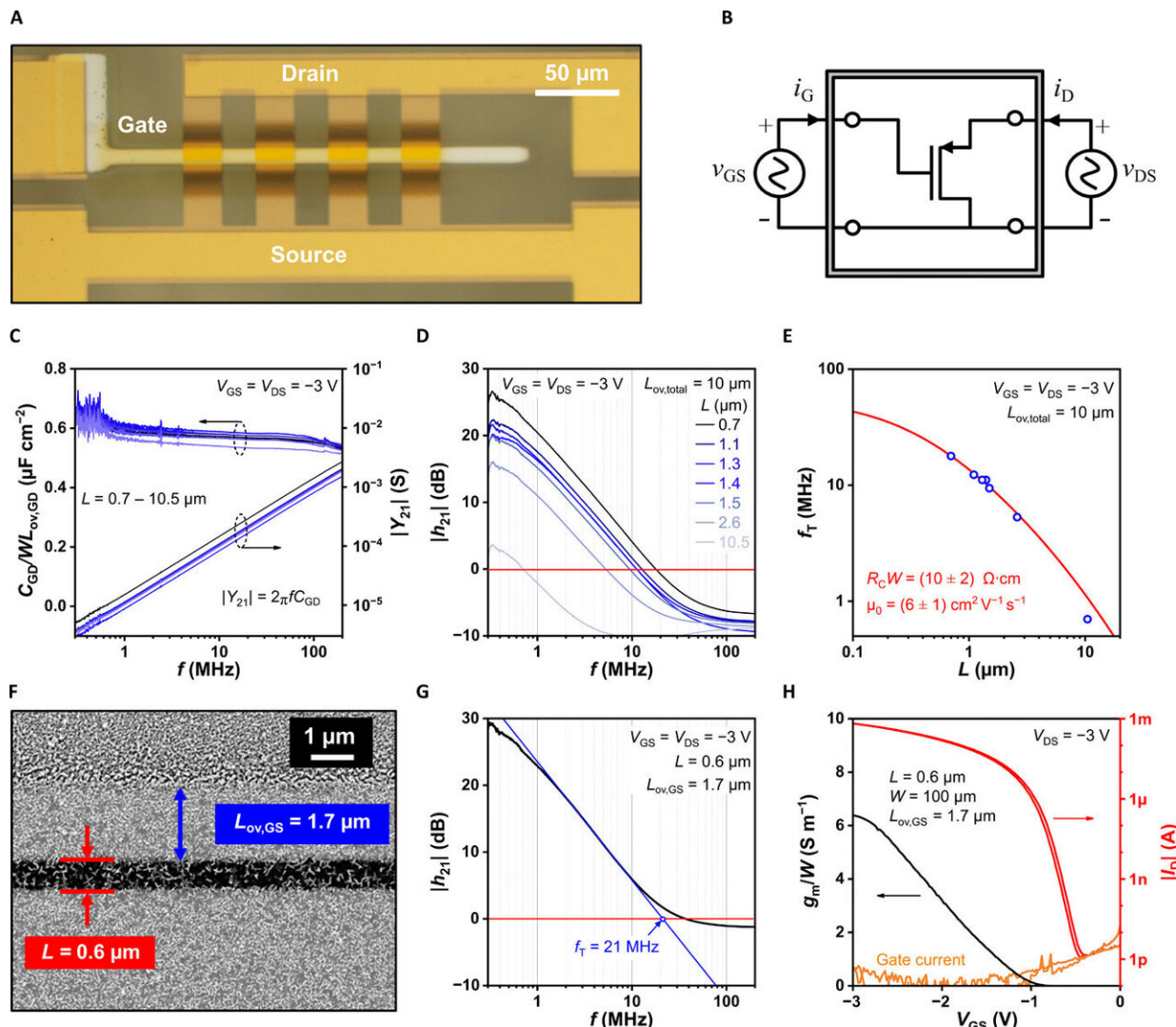
wave input signal with a frequency of 2 MHz, a duty cycle of 50%, and an amplitude of 2.5 V. Characteristic rise and fall time constants of the switching delays ( $\tau_{\text{rise}}$ ,  $\tau_{\text{fall}}$ ) were determined by fitting simple exponential functions to the measured output waveform. (D) Rise and fall time constants measured for supply voltages (VDD) of 1.5, 2.0, and 2.5 V. The amplitude of the square-wave input signal was identical to the supply voltage, and  $V_{\text{bias}} = -V_{\text{DD}}$  for each measurement. Credit: Science Advances, doi: 10.1126/sciadv.aaz5156

To understand the dynamic performance of the inverter, Borchert et al. applied a square-wave input signal with a frequency of 2 MHz and an amplitude of 1.5, 2.0 or 2.5 V. They detected the smallest time constants (19 and 56 nanoseconds—ns) for a supply voltage of 2.5 V and then summarized the results from the 11-stage ring oscillator. The team photographed the 11-stage ring oscillator circuit using [scanning electron microscopy](#) and measured its output signal. The signal-propagation delay in the setup was the smallest value reported to date (143 ns for a supply voltage of 1.6 V and 79 ns for a supply voltage of 4.4 V) at a supply voltage less than 50 V.



Dynamic circuit characteristics. (A) Circuit diagram and photograph of an 11-stage ring oscillator based on biased-load inverters fabricated on a PEN substrate. Photo credit: James W. Borchert, Max Planck Institute for Solid State Research. (B) SEM micrograph of the channel region of an individual C10-DNTT TFT in the ring oscillator. All TFTs in the circuit have a channel length ( $L$ ) of 1 μm and a total gate-to-contact overlap ( $L_{\text{ov, total}}$ ) of 4 μm. (C) Measured output signal of the ring oscillator operated with a supply voltage ( $V_{\text{DD}}$ ) of 4.4 V. A signal-propagation delay per stage ( $\tau$ ) of 79 ns is determined by fitting a sine wave to the output signal. (D) Stage delay and equivalent frequency ( $f_{\text{eq}} = 1/2\tau$ ) plotted as a function of the supply voltage. Credit: Science Advances, doi: 10.1126/sciadv.aaz5156

The team obtained more detailed information of the dynamic properties of individual TFTs using a [two-port network analysis](#). Using scattering-parameter (S-parameter) measurements the team studied the high-frequency characteristics of [organic TFTs](#). Based on the method, they performed detailed dynamic characterizations of thin film transistors and observed the area-normalized gate-drain capacitance to be constant with the frequency in all measurements. The scientists determined the transit frequencies and noted their dependence on the channel length to thereby extract the contact resistance and intrinsic channel mobility.



Two-port network analysis of flexible organic transistors. (A) Photograph of an organic TFT designed for two-port network analysis fabricated on a PEN substrate. All TFTs considered here have a total gate-to-contact overlap ( $L_{ov, total}$ ) of 10  $\mu\text{m}$  and a channel width ( $W$ ) of 100  $\mu\text{m}$ . Photo credit: James W. Borchert, Max Planck Institute for Solid State Research. (B) Circuit diagram of a two-port network with a TFT as the device under test. (C) Drain component of the total gate capacitance ( $CGD$ ) normalized by the gate-to-drain overlap area ( $WL_{ov, GD}$ ) and plotted as a function of the measurement frequency ( $f$ ) for all of the TFTs in the two-port network analysis. The gate-drain capacitance  $CGD$  was calculated from the measured admittance parameters ( $|Y_{21}| = 2\pi f CGD$ ). (D) Magnitude of the small-signal current gain ( $|h_{21}|$ ) of TFTs with channel lengths ( $L$ ) ranging from 0.7 to 10.5  $\mu\text{m}$  and with nominally identical gate-to-source and gate-to-drain overlaps ( $L_{ov, GS} = L_{ov, GD}$ ) plotted as a function of the measurement frequency. The transit frequencies ( $f_T$ ) are determined as the frequency at which  $|h_{21}| = 0 \text{ dB}$  (red line). (E) Transit frequency ( $f_T$ ) plotted as a function of the channel length ( $L$ ). The red line is a fit of Eq. 1 derived in the study to the measurement data (blue circles), yielding a width-normalized contact resistance ( $RCW$ ) of  $(10 \pm 2) \Omega \cdot \text{cm}$  and an intrinsic channel mobility ( $\mu_0$ ) of  $(6 \pm 1) \text{ cm}^2 \text{ V}^{-1} \text{ s}^{-1}$ . (F) SEM micrograph of the channel region of an asymmetric DPh-DNTT TFT with a channel length ( $L$ ) of 0.6  $\mu\text{m}$ , a gate-to-source overlap ( $L_{ov, GS}$ ) of 1.7  $\mu\text{m}$ , and a gate-to-drain overlap ( $L_{ov, GD}$ ) of 8.3  $\mu\text{m}$ . (G) Measured small-signal current gain ( $|h_{21}|$ ) of the same TFT plotted as a function of the measurement frequency, indicating a transit frequency ( $f_T$ ) of 21 MHz. (H) Measured transfer characteristics and transconductance ( $gm$ ) plotted as a function of the gate-source voltage of the same TFT. Credit: Science Advances, doi: 10.1126/sciadv.aaz5156

Parasitic fringe capacitance effects in the field-effect transistors could also arise when the semiconductor layer extended beyond the edges of the device. The team therefore reduced the gate-to-source overlap, while maintaining the total gate-to-contact overlap and the channel length constant to obtain a smaller total gate capacitance and a higher transit frequency. By optimizing the dimensions of the TFT, the scientists

obtained a transit frequency of 21 MHz as the highest value reported to date for an organic transistor made on a flexible substrate. The results demonstrated the possibility of building organic TFTs on flexible substrates with static and dynamic performance for [high-frequency](#) mobile electronic applications. The results of the work approached those of industry-standard low temperature [polycrystalline silicon TFTs](#), while using a TFT architecture that complied with existing industry-standard fabrication processes.

**More information:** James W. Borchert et al. Flexible low-voltage high-frequency organic thin-film transistors, *Science Advances* (2020). [DOI: 10.1126/sciadv.aaz5156](https://doi.org/10.1126/sciadv.aaz5156)

Kris Myny. The development of flexible integrated circuits based on thin-film transistors, *Nature Electronics* (2017). [DOI: 10.1038/s41928-017-0008-6](https://doi.org/10.1038/s41928-017-0008-6)

Xinge Yu et al. Metal oxides for optoelectronic applications, *Nature Materials* (2016). [DOI: 10.1038/nmat4599](https://doi.org/10.1038/nmat4599)

© 2020 Science X Network

Citation: Flexible low-voltage high-frequency organic thin-film transistors (2020, May 29) retrieved 12 January 2026 from <https://techxplore.com/news/2020-05-flexible-low-voltage-high-frequency-thin-film-transistors.html>

This document is subject to copyright. Apart from any fair dealing for the purpose of private study or research, no part may be reproduced without the written permission. The content is provided for information purposes only.